Bioinorganic Chemistry

Deutsche Ausgabe: DOI: 10.1002/ange.201505607
Internationale Ausgabe: DOI: 10.1002/anie.201505607

A Bioinspired Molybdenum Complex as a Catalyst for the Photo- and Electroreduction of Protons

Jean-Philippe Porcher, Thibault Fogeron, Maria Gomez-Mingot, Etienne Derat, Lise-Marie Chamoreau, Yun Li, and Marc Fontecave**

Abstract: *A molybdenum–dithiolene–oxo complex was prepared as a model of some active sites of Mo/W-dependent enzymes. The ligand, a quinoxaline–pyran-fused dithiolene, mimics molybdopterin present in these active sites. For the first time, this type of complex was shown to be active as a catalyst for the photoreduction of protons with excellent turnover numbers (500) and good stability in aqueous/organic media and for the electroreduction of protons in acetonitrile with remarkable rate constants (1030 s^{-1} at −1.3 V versus Ag/AgCl). DFT calculations provided insight into the catalytic cycle of the reaction, suggesting that the oxo ligand plays a key role in proton exchange. These results provide a basis to optimize this new class of H_2-evolving catalysts.*

Molybdenum (Mo) and tungsten (W) are present within the active sites of many enzymes that catalyze a variety of redox reactions.[1] One common active site has Mo/W coordinated to one or two molybdopterin (MPT) ligands (Figure 1). MPT is a highly unstable tricyclic organic molecule with a fused pyranopterin system and a dithiolene chelate moiety.

Mimicking sites of this type synthetically has been challenging. Pioneering investigations were reported by Holm and co-workers[2] over 20 years ago and were followed by others.[3] In general, simple dithiolene ligands were used. However, a report in 2009 used DFT calculations to show that in order to reproduce the molecular properties of MPT accurately, a simple dithiolene ligand was not appropriate even within a pyran ring and that the minimal ligand should be a fused pyran–tetrahydropyrazine-functionalized dithiolene, denoted prz (Figure 1).[4] Guided by this interesting study, we report herein the synthesis and characterization of an original bioinspired Mo complex **1** (Figure 1), using a quinoxaline–pyran-fused dithiolene ligand $qpdt^{2-}$ (**2**; Figure 1) which is closely related to MPT. It should be emphasized that the central pyrazine cycle within ligand **2** is oxidized with regard to the central tetrahydropyrazine cycle in the natural MPT ligand. No such Mo complex has been reported to date. However, a biomimetic Tp*Mo–pterin–dithiolene complex (Tp* = tris(3,5-dimethylpyrazolyl)hydroborate) has been previously prepared.[5]

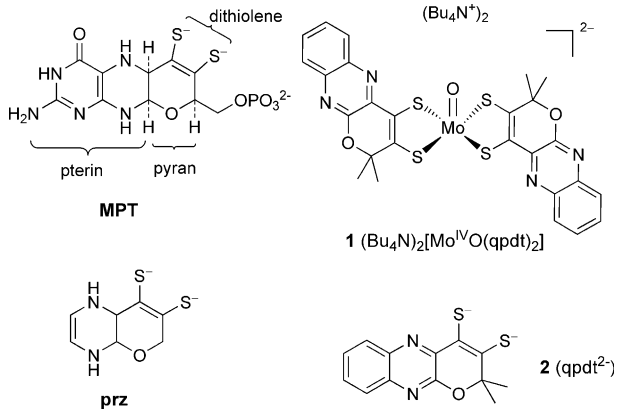

Figure 1. The structures of MPT, prz, the Mo^{IV} complex $(Bu_4N)_2[MoO(qpdt)_2]$ (**1**), and the ligand $qpdt^{2-}$ (**2**).

While Mo- and W-based enzyme active sites are involved in multielectron/multiproton catalytic processes, very little has been done to evaluate the potential of synthetic Mo- and W–dithiolene complexes as catalysts for the reduction of protons to hydrogen. Mo and W are nonprecious metals, relatively abundant and much cheaper than platinum. Although we recently reported the first study on W–dithiolene catalysts,[6] to our knowledge only one Mo–dithiolene homogeneous complex has been investigated and shown to display interesting H_2-evolving activities.[7] Co–dithiolene complexes have been more extensively studied as catalysts for proton reduction.[8] Herein, we show that complex **1** is an efficient and stable catalyst for converting protons into H_2 through electroreduction or photoreduction. DFT calculations give interesting insights into the catalytic cycle.

Owing to the instability of dithiolene derivatives, we chose to synthesize our ligand in the protected form **3** (Scheme 1). The tricyclic compound **5** (obtained from 2,3-dichloroquinoxaline in two steps with a total yield of 55%)[9] was hydrolyzed under acidic conditions to obtain **6** in excellent yield. Controlled monobromination of **6** at low temperature followed by triflation under standard conditions afforded **8**. Next, a double cross-coupling reaction was employed between **8** and two equivalents of $HSCH_2CH_2CO_2Et$ in the presence of a palladium catalyst $[Pd_2(dba)_3]$, a phosphine ligand (Xantphos), and iPr_2NEt.[10] The reaction afforded a mixture of products, containing **3** (77%), along with the

[*] J.-P. Porcher, T. Fogeron, Dr. M. Gomez-Mingot, Dr. Y. Li, Prof. M. Fontecave
Laboratoire de Chimie des Processus Biologiques
UMR 8229 CNRS, Collège de France, Université Paris 6
11 Place Marcelin Berthelot, 75231 Paris Cedex 05 (France)
E-mail: yun.xu-li@college-de-france.fr
marc.fontecave@college-de-france.fr
Dr. E. Derat, L.-M. Chamoreau
Sorbonne Universités, UPMC Université Paris 6
Institut Parisien de Chimie Moléculaire, UMR 8232 CNRS
4 place Jussieu, 75252 Paris Cedex 5 (France)

Supporting information for this article is available on the WWW under http://dx.doi.org/10.1002/anie.201505607.

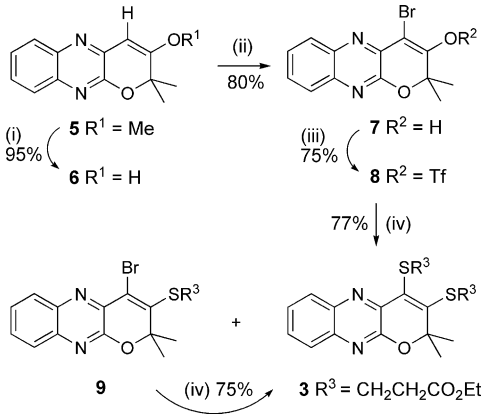

Scheme 1. Synthesis of **3**. Reagents and conditions: i) HCl (1 M), THF, RT; ii) Br_2, CH_2Cl_2, 0 °C; iii) Tf_2O, iPr_2NEt, CH_2Cl_2, RT; iv) $[Pd_2(dba)_3]$ (5%), Xantphos (10%), $HSCH_2CH_2CO_2Et$, iPr_2NEt, dioxane, 110 °C. Tf_2O = trifluoromethanesulfonic anhydride.

monosubstituted product **9** (8%), since vinyl triflate was more reactive than vinyl bromide. The isolated compound **9** was then transformed to **3** in 75% yield under the same conditions. The detailed synthetic procedure is described in the Supporting Information. Two comparable ligands have been reported.[11] However, the synthetic routes required several delicate steps with moderate yields, especially for the pyran-ring-closure step. Furthermore, no Mo/W complex was reported in these studies.

Compound **3** was treated with *t*BuOK under anaerobic conditions to generate the dithiolene ligand $qpdt^{2-}$ (**2**). This ligand was directly reacted with $K_3Na[MoO_2(CN)_4]\cdot 6H_2O$[12] under alkaline conditions at 45 °C for 30 minutes,[13] followed by cation exchange with Bu_4NBr, to afford the mononuclear complex $(Bu_4N)_2[Mo^{IV}O(qpdt)_2]$ (**1**) in 67% yield. As a result of the sensitivity of the complex to air, solid samples were kept within an anaerobic box.

Single crystals of **1** were obtained as dark-green plates by slow diffusion of Et_2O into a THF solution of the crude product in a glove box. An ORTEP diagram of the anionic component of **1** is shown in Figure 2. A summary of the crystal data collection and refinement parameters are listed in Table S1 in the Supporting Information.[14] Selected interatomic bond lengths and angles are listed in Table S2. **1** crystallizes in the orthorhombic system and the unit cell includes two mononuclear complexes and four Bu_4N^+ ions. The Mo^{IV} cation is pentacoordinated in a S_4O environment with a distorted square-based pyramidal geometry. The four dithiolene sulfur atoms originate from two symmetric *trans*-oriented $qpdt^{2-}$ ligands and the coordination sphere is completed with one terminal oxo ligand (O1). The Mo1 atom is located 0.755(1) Å above the average plane defined by the sulfur atoms S1, S2, S1′, and S2′. The Mo1–O1 length (1.694(2) Å) and Mo–S lengths (2.388(1) and 2.383(1) Å) are similar to those reported previously for bis(dithiolene)–$Mo^{IV}O$ complexes.[15] The deviation from 90° or 180° of bond angles around the Mo atom clearly indicates the significant distortion of the MoS_4O core from square-pyramidal geometry.

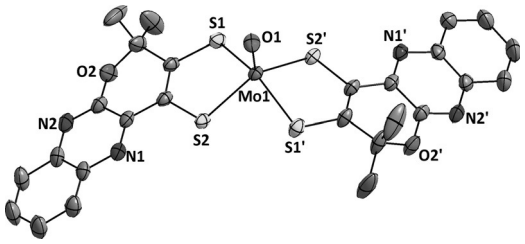

Figure 2. ORTEP diagram of $[Mo^{IV}O(qpdt)_2]^{2-}$ with partial atom labeling. Unlabeled atoms in the structure are carbon atoms. Thermal ellipsoids set at 50% probability. Hydrogen atoms and disorder are omitted for clarity.

Complex **1** is soluble in common solvents, such as THF, CH_3CN, and dimethylformamide (DMF), yielding yellow–green solutions that are highly sensitive to air. Its UV/Vis absorption spectrum in CH_3CN (Figure S1) shows four absorption maxima at $\lambda = 620$, 470, 385 and 320 nm with molar extinction coefficients $\varepsilon = 1178$, 30320, 15300, and 17400 $M^{-1}cm^{-1}$, respectively. In the IR spectrum, the ν(Mo=O) stretch at 905 cm^{-1} is similar to the one reported for $[Mo^{IV}O(C_2S_2COOMe_2)_2]$.[15] Compound **1** is diamagnetic (as evidenced by its ^1H NMR spectrum; Figure S2). The negative-ion electrospray mass spectrum in acetonitrile solution exhibits a peak cluster at $m/z = 661.95$, consistent with the molecular formula (Figure S3).

Complex **1** was studied for its catalytic light-assisted proton reduction activity under conditions comparable to those used in the case of $[Mo(bdt)_2(t\text{BuNC})_2]$ (bdt = benzene-1,2-dithiol).[7] Specifically, experiments were carried out in CH_3CN:H_2O (1:1) upon irradiation with visible light, using $[Ru(bpy)_3]^{2+}$ (bpy = 2,2′-bipyridine) as the photosensitizer and ascorbic acid (0.1 M, pH 4.0) as the sacrificial electron donor. H_2 production was monitored by GC analysis. The reaction rate was greatly dependent on the ratio of $[Ru(bpy)_3]^{2+}$/[**1**] (Figure S4), and a ratio value of 25 was used in subsequent experiments.

Figure 3 shows the time-dependent formation of H_2 during the photoreduction of protons catalyzed by complex **1** (5 μM). From these data, we extracted a remarkable initial turnover frequency (TOF) of 203 h^{-1} with respect to the catalyst (Figure 3, inset). In the absence of either **1**, $[Ru(bpy)_3]^{2+}$, or ascorbic acid, no H_2 was detected under the same conditions. Figure 3 shows that after about 5 h of irradiation, the rate of hydrogen evolution decreased significantly, indicating decomposition of at least one system component. After 15 h of reaction, it was found that addition of a solution of **1** was unable to restart H_2 production (Figure S5A). In contrast, addition of a solution of $[Ru(bpy)_3]^{2+}$ restored H_2 production to a large extent (Figure S5B). This result clearly shows that the system is mainly limited by the decomposition of the chromophore, as also observed by others,[7] and that the catalyst is relatively stable under these conditions.

The cyclic voltammogram of **1** in CH_3CN displays a reversible redox couple at −0.19 V versus the Ag/AgCl/KCl-saturated electrode assigned to the Mo^{IV}/Mo^{V} couple, one irreversible feature characteristic of dithiolene oxidation (0.62 V), and another redox process attributable to the reduction of Mo^{IV} (−2.0 V; Figure S6). The peak current at

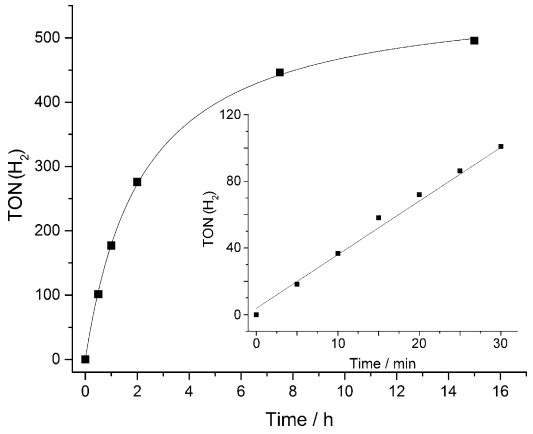

Figure 3. Light-driven hydrogen production in 1:1 H_2O:CH_3CN under a N_2 atmosphere at 20 °C. [ascorbic acid] = 0.1 M (pH 4.0); $[Ru(bpy)_3]^{2+}$/[**1**] = 25; [**1**] = 5 μM. Relative error is 10%. Inset: Initial rate determination. TON = turnover number.

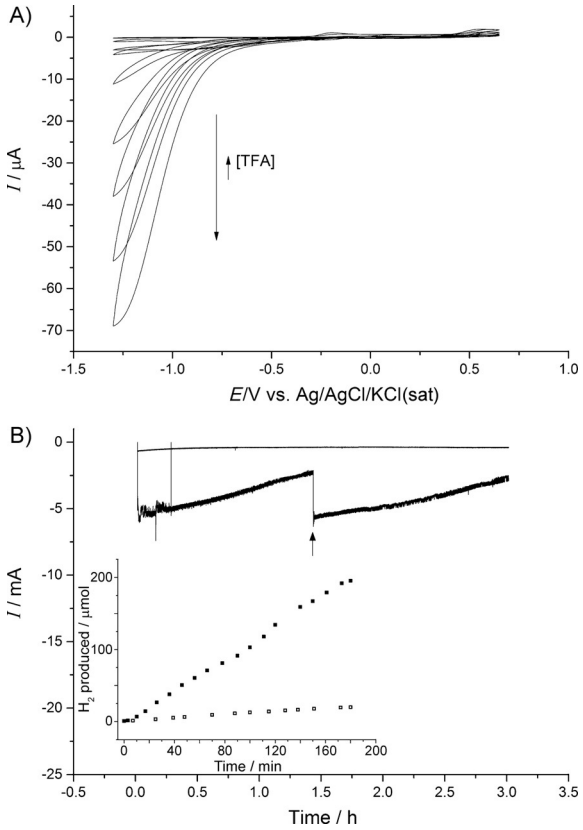

Figure 4. A) Cyclic voltammograms of 1 mM of complex **1** in 0.1 M tetra-*n*-butylammonium perchlorate (TBAP) in CH_3CN in the presence of increasing concentrations of TFA (0–125 mM). In all cases, the third scan is shown. The current of the catalytic wave (half-wave potential circa −0.95 V) becomes more intense with increasing [TFA]. Scan rate 50 $mV s^{-1}$; glassy carbon electrode. B) Current passed as a function of time during electrolysis at −1.3 V of 0.5 mM of complex **1** in the presence of 50 mM TFA (bottom line). After 1.5 h, a further 50 mM of TFA (100 equiv) was added (black arrow). Top line: the same experiment in the absence of catalyst. Inset: H_2 production as a function of time during electrolysis of 50 mM TFA in the absence (empty squares) or in the presence (dark squares) of complex **1**.

−0.19 V displays a linear relation to the square root of the scan rate, proving a diffusion-controlled electrochemical process typical for molecular catalysts (Figure S7). Addition of increasing amounts of trifluoroacetic acid (TFA) triggers the appearance of a catalytic wave that grows with an onset potential at −0.55 V and a half-wave potential of −0.95 V, corresponding to an overpotential of 700 mV[16] (Figure 4 A). A prewave also appears at −0.75 V and shifts towards positive potentials with constant current intensity with increasing additions of acid and is assigned to a Mo^{IV}/Mo^{III} transition. A shift on the peak potential is also observed for the Mo^{IV}/Mo^{V} couple upon addition of TFA (Figure S8A), which can be reversed upon subsequent neutralization with Et_3N (Figure S8B).

These electrochemical data suggest that a reversible protonation process greatly facilitates the reduction of **1**. Electrodeposits as potential catalysts are excluded on the basis of negative standard rinse experiments. Quantitative analysis of the cyclic voltammograms allowed us to determine a TOF value of 1030 s^{-1} at −1.3 V versus Ag/AgCl using 0.1 M TFA (Figure S9 and S10). Electrolysis at a controlled potential (−1.3 V) confirms that the observed current enhancements correspond to the formation of H_2 (Figure 4 B). Using 100 equivalents of TFA, the current, initially at 6 mA for about 30 minutes, slowly decayed as a consequence of TFA consumption. Indeed, addition of TFA (100 equiv) after 1.5 hours restored the current intensity which then again slowly decayed, illustrating the stability of the catalyst under these conditions. After a short lag phase of about 5 minutes, H_2 production occurred linearly as a function of time. Within this lag phase, the charge passed through the system accounted for 2 electrons required to activate the catalyst prior to H_2 evolution. Faradic yields after 1.5 h and 3 h were 92% and 86%, respectively. In the absence of catalyst, current intensities were below 0.4 mA.

DFT calculations were performed with Turbomole at the B3LYP-D3/def2-SV(P) level (see the Supporting Information) to explore possible reaction pathways for H_2 evolution catalyzed by compound **1**. This method has already been used for comparable systems.[17] As shown in Figure S11 and S12, protonation occurs preferentially at one of the N atoms of the ligand with respect to the oxo group (−27.32 kcal mol^{-1} versus −12.61 kcal mol^{-1}). This reaction facilitates the first one-electron reduction (−16.49 kcal mol^{-1} versus 5.26 kcal mol^{-1}). The next steps of the process involved protonation at the oxo group, a second one-electron reduction (slightly more favorable than the first), and protonation to generate a hydride species. Intramolecular protonation of the hydride affords H_2 via a localized transition state with a barrier of 20.39 kcal mol^{-1}. This value is slightly larger than that found for W–dithiolene complexes.[6] A catalytic cycle for this process is shown in Scheme 2.

The photoreduction process was also studied using DFT calculations combining the $[Ru(bpy)_3]^{2+}$ photosensitizer (PS) and the protonated catalyst (Figure S13). After photoexcitation, the PS is in a triplet excited state with one unpaired electron localized on the d_{z^2} orbital of Ru and one unpaired electron on the π system of the bpy ligand. The protonated complex **1** can accept electrons onto its LUMO, localized on the π system of the dithiolene moieties. DFT calculations

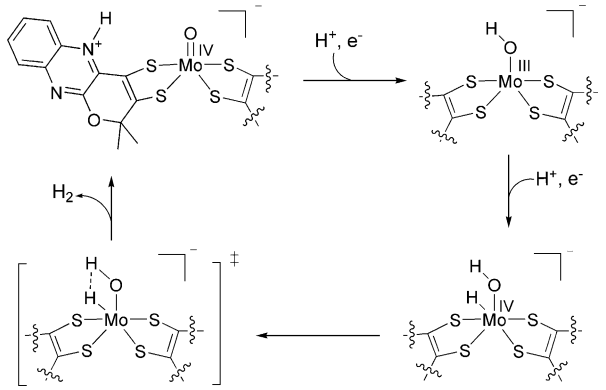

Scheme 2. Proposed catalytic cycle for proton reduction by complex **1**.

showed a spontaneous electron transfer as a result of the favorable π–π stacking interaction between the two planar aromatic moieties (bpy and qpdt). After electron transfer, one electron is found to be on the Mo center ($d_{x^2-y^2}$ orbital) while the other one is found on the bpy ligand. The electron transfer thus occurs first from the metal of the excited $[Ru(bpy)_3]^{2+*}$ to the dithiolene ligand on complex **1** (intermolecular metal-to-ligand charge transfer, MLCT) and then from the ligand to the Mo atom (intramolecular ligand-to-metal charge transfer, LMCT).

We have presented herein a novel Mo–oxo complex which has two dithiolene ligands closely related to the biological ligand molybdopterin (MPT). The complex is active for the photocatalytic reduction of protons with excellent turnover numbers (500) and TOFs (203 h^{-1}) and has very good stability in aqueous/organic media. Complex **1** is also a very good catalyst for the electroreduction of protons in acetonitrile with a low onset potential and a remarkable TOF value (1030 s^{-1} at −1.3 V versus Ag/AgCl). Finally, DFT calculations provided interesting insights into the catalytic cycle of the reaction, which could serve as a basis for further improvement of these catalysts. First, calculations showed that the ligand provides a proton exchange site, namely one N atom, which facilitates subsequent reductions. Second, they suggested that the Mo–oxo moiety reacts with two electrons and two protons to form a reactive hydrido $[Mo^{IV}OH(H)(LH)(L)]$ intermediate. Thus, the oxo ligand plays a key role in facilitating protonation of the hydride and in further H_2 formation. This complex provides a starting point for further biomimetic studies through modification of the ligand and the coordination sphere, leading to the preparation and application of more biologically relevant Mo-based catalysts.

Acknowledgements

This work was supported by the French National Research Agency (CarBioRed ANR-12-BS07-0024-03), the Fondation de l'Orangerie for individual Philanthropy, the French State Program "Investissements d'Avenir" (Grants "LABEX DYNAMO", ANR-11-LABX-0011). We thank L. Dubost and the Muséum National d'Histoire Naturelle for technical support and P. Simon for H_2 detection methods.

Keywords: density functional calculations · dithiolene ligands · homogeneous catalysis · hydrogen evolution reaction · molybdenum

How to cite: *Angew. Chem. Int. Ed.* **2015**, *54*, 14090–14093
Angew. Chem. **2015**, *127*, 14296–14299

[1] a) R. J. P. Williams, J. J. R. F. Da Silva, *Biochem. Biophys. Res. Commun.* **2002**, *292*, 293–299; b) R. Hille, J. Hall, P. Basu, *Chem. Rev.* **2014**, *114*, 3963–4038; c) M. J. Romão, *Dalton Trans.* **2009**, 4053–4068; d) L. B. Maia, J. J. G. Moura, I. Moura, *J. Biol. Inorg. Chem.* **2015**, *20*, 287–309.
[2] a) J. H. Enemark, J. J. A. Cooney, J.-J. Wang, R. H. Holm, *Chem. Rev.* **2004**, *104*, 1175–1200; b) S. Groysman, R. H. Holm, *Inorg. Chem.* **2007**, *46*, 4090–4102; c) B. S. Lim, J. P. Donahue, R. H. Holm, *Inorg. Chem.* **2000**, *39*, 263–273.
[3] a) P. Basu, S. J. N. Burgmayer, *J. Biol. Inorg. Chem.* **2015**, *20*, 373–383; b) C. Schulzke, *Eur. J. Inorg. Chem.* **2011**, 1189–1199; c) H. Sugimoto, H. Tsukube, *Chem. Soc. Rev.* **2008**, *37*, 2609–2619; d) A. Majumdar, S. Sarkar, *Coord. Chem. Rev.* **2011**, *255*, 1039–1054.
[4] U. Ryde, C. Schulzke, K. Starke, *J. Biol. Inorg. Chem.* **2009**, *14*, 1053–1064.
[5] B. R. Williams, Y. C. Fu, G. P. A. Yap, S. J. N. Burgmayer, *J. Am. Chem. Soc.* **2012**, *134*, 19584–19587.
[6] M. Gomez-Mingot, J.-P. Porcher, T. K. Todorova, T. Fogeron, C. Mellot-Draznieks, Y. Li, M. Fontecave, *J. Phys. Chem. B* **2015**, DOI: 10.1021/acs.jpcb.5b01615.
[7] W. T. Eckenhoff, W. W. Brennessel, R. Eisenberg, *Inorg. Chem.* **2014**, *53*, 9860–9869.
[8] Z. J. Han, R. Eisenberg, *Acc. Chem. Res.* **2014**, *47*, 2537–2544.
[9] D. E. Ames, J. C. Mitchell, C. C. Takundwa, *J. Chem. Res. Miniprint* **1985**, 1683–1696.
[10] T. Itoh, T. Mase, *Org. Lett.* **2004**, *6*, 4587–4590.
[11] a) L. Marbella, B. Serli-Mitasev, P. Basu, *Angew. Chem. Int. Ed.* **2009**, *48*, 3996–3998; *Angew. Chem.* **2009**, *121*, 4056–4058; b) B. Bradshaw, A. Dinsmore, W. Ajana, D. Collison, C. D. Garner, J. A. Joule, *J. Chem. Soc. Perkin Trans. 1* **2001**, 3239–3244.
[12] J. P. Smit, W. Purcell, A. Roodt, J. G. Leipoldt, *Polyhedron* **1993**, *12*, 2271–2277.
[13] a) A. Döring, C. Fischer, C. Schulzke, *Z. Anorg. Allg. Chem.* **2013**, *639*, 1552–1558; b) E. S. Davies, R. L. Beddoes, D. Collison, A. Dinsmore, A. Docrat, J. A. Joule, C. R. Wilson, C. D. Garner, *J. Chem. Soc. Dalton Trans.* **1997**, 3985–3995.
[14] CCDC 1405606 (**1**) contains the supplementary crystallographic data for this paper. These data can be obtained free of charge from The Cambridge Crystallographic Data Centre. Crystal data for **1** (black prismatic crystals): $C_{58}H_{92}MoN_6O_3S_4$, $P2_12_12$, $a=16.4749(4)$, $b=20.9704(6)$, $c=8.9274(2)$ Å, $V=3084.28(13)$ Å^3, $Z=2$, $T=200(2)$ K, $\mu=1.233$ mm^{-1}, 35002 reflections measured, 9006 independent ($R_{int}=0.0197$), 8445 observed [$I\geq 2\sigma(I)$], 339 parameters, final R indices R_1 [$I\geq 2\sigma(I)$] = 0.0286 and wR_2 (all data) = 0.0721, GOF on $F^2=1.033$, max/min residual electron density = 0.509/−0.300 e Å^{-3}.
[15] D. Coucouvanis, A. Hadjikyriacou, A. Toupadakis, S. M. Koo, O. Ileperuma, M. Draganjac, A. Salifoglou, *Inorg. Chem.* **1991**, *30*, 754–767.
[16] V. Fourmond, P. A. Jacques, M. Fontecave, V. Artero, *Inorg. Chem.* **2010**, *49*, 10338–10347.
[17] N. R. M. Leopoldini, M. Toscano, M. Dulak, T. A. Wesolowski, *Chem. Eur. J.* **2006**, *12*, 2532–2541.

Received: June 17, 2015
Revised: July 18, 2015
Published online: September 25, 2015

